

Ambipolar diffusion theory of the hot-cathode negative glow

J. H. Ingold

GE Lighting, General Electric Company, Cleveland, Ohio 44112

(Received 9 July 1990)

Ambipolar diffusion theory of the negative glow (NG) and Faraday dark space (FDS) of a cylindrical gas discharge maintained by thermionic emission from a hot cathode is discussed. Electrons are divided into two groups: thermionic beam electrons and plasma electrons. Radial diffusion losses are handled by introducing the usual diffusion length. Inputs to the model include probabilities of excitation and ionization by thermionic beam electrons and by plasma electrons, electron and ion temperatures and mobilities, and discharge tube radius. The model predicts the following measured quantities with good qualitative agreement: (a) combined length of NG plus FDS, (b) axial distribution of plasma electron density, and (c) ion current to cathode. The model also predicts two reversals in axial electric field: one in the NG near the cathode where axial current is supported by ambipolar diffusion, and one near the end of the FDS at the beginning of the positive column where axial current can no longer be supported by ambipolar diffusion.

I. INTRODUCTION

This paper deals with ambipolar diffusion theory of the negative glow (NG) and Faraday dark space (FDS) of a cylindrical gas discharge maintained by thermionic emission from a hot cathode. The basic features of the hot-cathode glow discharge can be summarized as follows.¹ Thermionic electrons are accelerated through the cathode fall (CF) without collisions into a relatively field-free NG, where they undergo elastic and inelastic collisions with other particles. The potential difference across the CF is generally on the order of the ionization potential of the gas, and CF thickness is generally on the order of 0.01 cm because of the relatively high ion-current density impinging on the cathode. Consequently, thermionic electrons in the hot-cathode NG are monoenergetic, with energy equal to the CF potential. Inelastic collisions between these energetic electrons and atoms produce excited atoms, ions, and low-energy electrons, forming a low-energy plasma.

The strength of the ionization source is large enough to provide ambipolar diffusion losses in the radial as well as the axial direction. Axial current in the NG and FDS is supported by ambipolar diffusion. The positive column (PC) begins when the plasma generated by the ionization source has been dissipated by ambipolar diffusion losses in the radial direction.

Ambipolar diffusion theory, which has been used so successfully to explain the PC,^{2,3} is valid whenever the Debye length is small compared with a characteristic dimension of the discharge tube.⁴ When this criterion is met, then there is a low-field region which is nearly electrically neutral occupying most of the central region of the discharge tube, and there is a high-field region which is ion rich near the insulating wall, resulting from the necessity to hold back the much more mobile electrons. The Debye length varies as the square root of the ratio of electron temperature to electron density,⁵ so that a small

Debye length occurs when the electron temperature is low and the electron density is high. In what follows, assumptions and basic equations of ambipolar diffusion theory as applied to the hot-cathode NG and FDS are given. Then a qualitative model which predicts the important features observed⁶ in the hot-cathode glow discharge is discussed, and good qualitative agreement between theory and observation is established.

II. THEORY

A. Assumptions

Visual observation of the cathode region of a hot-cathode discharge in a cylindrical tube containing a mixture of mercury vapor and rare gas shows the NG extending for about one tube radius in all directions about the oxide cathode, and the FDS extending for a length somewhat smaller than one tube diameter to the PC.⁷ No cathode dark space is visible, presumably because it is so thin that it cannot be distinguished by the unaided eye. The axial potential distribution in such a discharge tube is sketched in Fig. 1. The electric field is high in the CF because the CF potential drop is on the order of the lowest ionization potential of the gases in the discharge tube, and because the CF is very thin due to high ion-current density impinging on the cathode. In fact, the electric field in the CF region is so high, and CF thickness so small, that energetic electrons are injected into the NG with an average energy equal to the CF potential drop. In this paper, these energetic electrons are called *beam* electrons, to distinguish them from low-energy electrons, called *plasma* electrons, which are produced by ionization of the gases in the discharge tube by beam electrons.

There are three processes by which beam electrons lose energy in the NG: (1) elastic collisions with atoms; (2) inelastic collisions with atoms, i.e., excitation and ioniza-

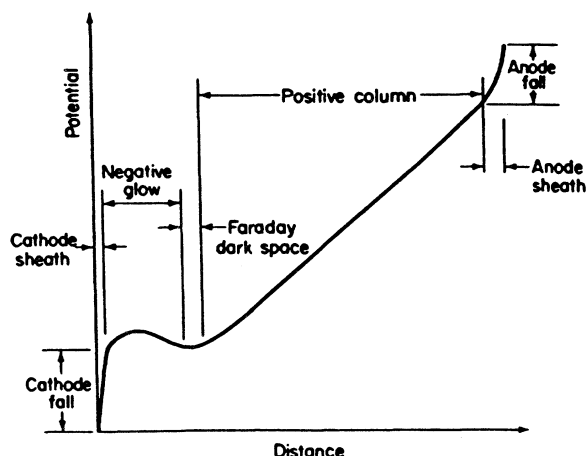


FIG. 1. Sketch of axial potential distribution in a long cylindrical discharge tube (reprinted from Ref. 7 by permission of the author).

tion; and (3) thermalizing collisions with plasma electrons. In Appendix II of Ref. 6, it is argued that process 2 is much more important than process 1 or process 3 in the typical hot-cathode NG. Therefore, energy losses due to processes other than inelastic collisions between beam electrons and atoms can be neglected. Having undergone an inelastic collision, however, a beam electron loses a large fraction of its energy, and is therefore converted from the beam population n_b to the plasma population n_p .

In the PC of a typical mercury plus rare-gas discharge, the electron temperature is about 12 000 K and the radially averaged electron density is about $2 \times 10^{11} \text{ cm}^{-3}$,⁸ giving a Debye length of about $2 \times 10^{-3} \text{ cm}$, which is much smaller than the tube radius of about 1.8 cm. Therefore, it can be assumed that the PC of this discharge is controlled by ambipolar diffusion. According to measurement,⁶ the electron temperature in the NG is about the same as that in the PC, and the electron density is somewhat higher, so that it is reasonable to assume that the NG is also controlled by ambipolar diffusion.

These considerations lead to the following list of assumptions on which the theory of the hot-cathode NG controlled by ambipolar diffusion is based.

(1) Following Ref. 6, it is assumed that thermionic electrons are accelerated through the CF without collision. Once in the NG, a beam electron retains the CF energy until it undergoes an inelastic collision, a process in which the beam electron itself becomes a low-energy plasma electron and an additional electron-ion pair may be formed.

(2) The role of elastic collisions between beam electrons and gas atoms in the NG is to randomize momentum but not energy of the beam electrons, resulting in a sort of spherical shell for the velocity distribution.⁹ The shell moves forward in the axial direction with an average velocity smaller than the mean speed represented by the radius of the shell, which is proportional to the square root

of the cathode fall of potential. The forward motion is a result of diffusion due to a strong concentration gradient caused by depletion of the beam.

(3) It is assumed that plasma electron density n_p is much higher than the beam electron density n_b in the NG. This assumption is based on the argument that the average velocity of beam electrons is much higher than that of plasma electrons; therefore, plasma density is much higher than beam density, because each species carries about the same current—beam electrons carry current in the CF, and plasma electrons in the NG.

(4) The NG plasma is assumed to be neutral, i.e., $n_e = n_i \equiv n_p$.

(5) For simplicity, radial variations in densities and fields are suppressed by the standard technique of introducing a diffusion length $\Lambda \equiv R/2.405$ to account for radial diffusion loss of electron and ions. In this relation, R is the radial extent of the discharge and 2.405 is the first value of λ in the equation $J_0(\lambda) = 0$, where J_0 is a zero-order Bessel function of the first kind.

(6) Plasma electron current density is assumed to be zero at the cathode end of the NG, because plasma electrons cannot stream against the CF sheath, and no plasma electrons are emitted by the CF sheath.

(7) Plasma density and ion-current density are assumed to satisfy the Bohm relation¹⁰ at the cathode end of the NG, i.e., ion velocity is equal to the Bohm velocity.¹¹

(8) Plasma density n_p is assumed to decrease monotonically in the axial direction due to radial ambipolar diffusion.¹²

(9) Ion-current density is assumed to be zero at the PC end of the FDS. This assumption is based on the argument that ion-current density is positive in the FDS and negative in the PC; therefore, it must be zero at the boundary between the FDS and PC.

B. Equations

1. Beam electrons n_b

According to assumptions 1 and 2, the behavior of beam electrons is governed by the following continuity and diffusion equations:⁶

$$\frac{d\Gamma_b}{dz} = -v_b n_b, \quad \Gamma_b = -D_b \frac{dn_b}{dz},$$

where z is axial distance from the beginning of the NG, Γ_b is current density of beam electrons, D_b is the diffusion coefficient of beam electrons, and v_b is the frequency of inelastic collisions by beam electrons. The latter is the sum of excitation frequency ν_{xb} and ionization frequency ν_{ib} . D_b and v_b are independent of position by reason of assumption 1.

These two equations can be combined to give the following diffusion equation for beam electrons:

$$\frac{d^2 n_b}{dz^2} - \alpha_b^2 n_b = 0, \quad \alpha_b^2 \equiv \frac{v_b}{D_b},$$

which has the solution

$$n_b(z) = n_{b0} \exp(-\alpha_b z),$$

where n_{b0} is the value of n_b at $z=0$, the beginning of the NG. The exponential decrease in the axial direction given by this equation has been observed.⁶

Beam current density falls exponentially according to the equation

$$\Gamma_b(z) = D_b n_{b0} \alpha_b \exp(-\alpha_b z) = \Gamma_{b0} \exp(-\alpha_b z), \quad (1)$$

where

$$n_{b0} \equiv \frac{\Gamma_{b0}}{D_b \alpha_b}.$$

Average velocity v_b of beam electrons, due to the diffusion current density Γ_b , is given by the relation $v_b = D_b \alpha_b$, while the mean speed of beam electrons is equal to $(2eV_k/m)^{1/2}$, where V_k is the CF potential and e/m is the charge-to-mass ratio of the electron.

2. Plasma electrons and ions n_p ($n_e = n_i \equiv n_p$)

According to assumptions 3–5, the behavior of plasma electrons (subscript e) and ions (subscript i) is governed by the following continuity and diffusion equations:

$$\begin{aligned} \frac{d\Gamma_e}{dz} &= (1+f_{ib})v_b n_b - (D_a \Lambda^{-2} - v_{ip})n_p, \\ \frac{d\Gamma_i}{dz} &= f_{ib}v_b n_b - (D_a \Lambda^{-2} - v_{ip})n_p, \\ \frac{\Gamma_e}{\mu_e} &= -\theta_e \frac{dn_p}{dz} + n_p E, \quad \frac{\Gamma_i}{\mu_i} = -\theta_i \frac{dn_p}{dz} - n_p E, \end{aligned} \quad (2)$$

where f_{ib} is defined as the ratio of ionization frequency ν_{ib} to total inelastic collision frequency ν_b of beam electrons, i.e.,

$$f_{ib} \equiv \frac{\nu_{ib}}{\nu_{xb} + \nu_{ib}},$$

and the other symbols have their usual meanings— D_a is the ambipolar diffusion coefficient, E is electric field (defined as the positive gradient of potential V), μ is mobility, θ is temperature expressed in volts, and v_{ip} is the frequency of ionization by plasma electrons. The first term on the right side of each continuity equation expresses the assumption that an ionization event by a beam electron produces two plasma electrons and one ion. The second term on the right side of each accounts for wall losses by ambipolar diffusion. The third term on the right side of each accounts for ionization by plasma electrons, each event of which produces one additional plasma electron and one additional ion. In the PC, the condition for a steady state to obtain is $v_{ip} = D_a / \Lambda^2$, which will be recognized as the Schottky condition.² Because the NG can be maintained entirely by beam electrons, as shown later, it is not necessary that the Schottky condition be fulfilled in the NG.

The last two equations can be combined to give

$$\begin{aligned} \frac{dn_p}{dz} &= -\frac{1}{\theta_e + \theta_i} \left[\frac{\Gamma_e}{\mu_e} + \frac{\Gamma_i}{\mu_i} \right], \\ n_p E &= \frac{1}{\theta_e + \theta_i} \left[\frac{\theta_i \Gamma_e}{\mu_e} - \frac{\theta_e \Gamma_i}{\mu_i} \right]. \end{aligned} \quad (3)$$

By differentiation of the first of these equations and elimination of Γ_e and Γ_i by means of the continuity equations, the following diffusion equation for plasma electrons and ions is obtained:

$$\frac{d^2 n_p}{dz^2} - k_p^2 n_p = -\frac{\Gamma_{b0}}{\theta_e + \theta_i} \left[\frac{1+f_{ib}}{\mu_e} + \frac{f_{ib}}{\mu_i} \right] \alpha_b \exp(-\alpha_b z),$$

where

$$k_p^2 \equiv \Lambda^{-2} - \alpha_p^2, \quad \alpha_p^2 \equiv \frac{v_{ip}}{D_a}.$$

This diffusion equation can be solved in terms of elementary functions. When the conditions expressed by assumptions 6–8 are imposed, then the solutions for plasma particle densities and plasma current densities are the following:

$$\begin{aligned} n_p(z) &= \frac{f_{ib}\mu_e + (1+f_{ib})\mu_i}{\mu_e + \mu_i} \frac{\alpha_b}{(\alpha_b^2 - k_p^2)} \frac{\Gamma_{b0}}{D_a} \\ &\quad \times [A \exp(-k_p z) - \exp(-\alpha_b z)], \\ \frac{\Gamma_e(z)}{\Gamma_{b0}} &= (1+f_{ib}) [1 - \exp(-\alpha_b z)] \\ &\quad - \frac{f_{ib}\mu_e + (1+f_{ib})\mu_i}{\mu_e + \mu_i} \frac{\alpha_b k_p}{\alpha_b^2 - k_p^2} \\ &\quad \times \left[A [1 - \exp(-k_p z)] \right. \\ &\quad \left. - \frac{k_p}{\alpha_b} [1 - \exp(-\alpha_b z)] \right], \end{aligned} \quad (4)$$

and

$$\frac{\Gamma_i(z)}{\Gamma_{b0}} = \frac{\Gamma_{i0}}{\Gamma_{b0}} + \frac{\Gamma_e(z)}{\Gamma_{b0}} - 1 + \frac{\Gamma_b(z)}{\Gamma_{b0}}, \quad (5)$$

where

$$A \equiv \frac{1 + (1 + \mu_i/\mu_e) D_a \alpha_b / v_B}{1 + (1 + \mu_i/\mu_e) D_a k_p / v_B}, \quad v_B \equiv \left[\frac{e(\theta_e + \theta_i)}{m_i} \right]^{1/2}, \quad (6)$$

and

$$\begin{aligned} \frac{\Gamma_{i0}}{\Gamma_{b0}} &= -\frac{f_{ib} + (1+f_{ib})\mu_i/\mu_e}{1 + (1 + \mu_i/\mu_e) D_a k_p / v_B} \frac{\alpha_b}{\alpha_b + k_p} \\ &\approx \frac{f_{ib} \alpha_b}{\alpha_b + k_p}. \end{aligned} \quad (7)$$

The combined length of NG + FDS, denoted by L , is found by imposing the condition of assumption 9—

namely, $\Gamma_i(L)=0$ —on Eq. (5).

The constant A differs little from unity, because the ratios μ_i/μ_e , $D_a\alpha_b/v_B$, and D_ak_p/v_B are small compared with unity. Therefore, the solutions for plasma density and current densities are changed but slightly if assumption 7 is changed to $n_p(0)=0$, making $A \equiv 1$.

According to Eq. (4) and the relation

$$n_b(z) = \frac{\Gamma_{b0}}{D_b\alpha_b} \exp(-\alpha_b z),$$

the ratio n_p/n_b satisfies the inequality

$$\frac{n_p}{n_b} \geq f_{ib} \frac{\alpha_b}{\alpha_b + k_p} \frac{v_b}{v_B}.$$

According to Sec. II C, the term on the right of this inequality is approximately equal to 40 for the conditions of the experiments described in Ref. 6. The equality sign holds at $z=0$, and the left side of this inequality increases rapidly with increasing z , which is justification for assumption 3.

C. Transport and rate coefficients

In Sec. III of this paper, calculated results are presented for the case investigated experimentally in Ref. 6—namely, a discharge in 1 Torr neon and 6 mTorr mercury. The transport and rate coefficients used for the calculations are given in this section.

1. Beam electrons

The mercury ionization frequency for beam electrons with energy ξ is expressed by the formula

$$\nu_{ib} = n_{\text{Hg}} Q_i(\xi) \bar{v}_b(\xi),$$

where n_{Hg} is mercury density, $\bar{v}_b \equiv (2e\xi/m)^{1/2}$ is the mean speed of beam electrons, and $Q_i(\xi)$ is mercury ionization cross section, expressed in units of cm^2 by the relation

$$Q_i(\xi) = 4.95 \times 10^{-16} [\ln(\xi/10.4)]^{1/2}$$

for energy $\xi \geq 10.4$ V. This relation is based on the measurement of Ref. 13.

The mercury excitation frequency for beam electrons is expressed by the formula

$$\nu_{xb} = n_{\text{Hg}} Q_x(\xi) \bar{v}_b(\xi),$$

where the total mercury excitation cross section $Q_x(\xi)$ is expressed in units of cm^2 by the relation

$$Q_x(\xi) = 1.6 \times 10^{-16} (\xi - 4.7)^{0.43}$$

for energy $\xi \geq 4.7$ V. This relation is based on the mercury excitation cross sections of Ref. 14.

The diffusion coefficient for beam electrons is given by the expression

$$D_b = \frac{\bar{v}_b(\xi)}{3n_{\text{Ne}} Q_m(\xi)},$$

where $n_{\text{Ne}} = 3.23 \times 10^{16} \text{ cm}^{-3}$ is the neon density at 1

Torr and 293 K, and Q_m is the momentum-transfer cross section for electrons scattered by neon atoms.¹⁵ In the present work, $Q_m(\xi)$ is approximated by $1.62 \times 10^{-16} \xi^{0.152} \text{ cm}^2$ for ξ greater than 1 V, and by $1.62 \times 10^{-16} \xi^{0.366} \text{ cm}^2$ for ξ less than 1 V. For $\xi = 15$ V and $n_{\text{Ne}} = 3.23 \times 10^{16} \text{ cm}^{-3}$, this equation gives $D_b = 1 \times 10^7 \text{ cm}^2 \text{ sec}^{-1}$.

These relations lead to the following expression for α_b :

$$\alpha_b = [3P_c(P_x + P_i)]^{1/2},$$

where $P_c \equiv n_{\text{Ne}} Q_m$, $P_x \equiv n_{\text{Hg}} Q_x$, and $P_i \equiv n_{\text{Hg}} Q_i$, similar to Ref. 6. For example, when $\xi = V_k = 15$ V, $n_{\text{Hg}} = 1.85 \times 10^{14} \text{ cm}^{-3}$, and $n_{\text{Ne}} = 3.23 \times 10^{16} \text{ cm}^{-3}$, then this expression gives $\alpha_b = 1.89 \text{ cm}^{-1}$, in fair agreement with the measured value of 1.82 cm^{-1} .⁶

2. Plasma particles

Ion temperature θ_i is taken to be 0.027 V, corresponding to a gas temperature of 313 K. Plasma electron temperature θ_e is taken as an adjustable parameter, reflecting the absence of an energy-balance equation for determination of θ_e .

Ion mobility is given by the relation

$$\mu_i = \mu_{i0} \frac{2.69 \times 10^{19}}{n_{\text{Ne}}},$$

where the value $\mu_{i0} = 6 \text{ cm}^2 \text{ V}^{-1} \text{ sec}^{-1}$ is taken from Ref. 16. For $n_{\text{Ne}} = 3.23 \times 10^{16} \text{ cm}^3$, this equation gives $\mu_i = 5000 \text{ cm}^2 \text{ V}^{-1} \text{ sec}^{-1}$.

Plasma electron mobility is given by the relation

$$\mu_e(\theta_e) = \frac{\bar{v}_e}{3n_{\text{Ne}} Q_m(3\theta_e/2)\theta_e},$$

where $\bar{v}_e = (8e\theta_e/\pi m)^{1/2}$ is the mean speed of electrons with a Maxwellian velocity distribution. For $\theta_e = 1$ V and $n_{\text{Ne}} = 3.23 \times 10^{16} \text{ cm}^{-3}$, this equation gives $\mu_e = 4 \times 10^6 \text{ cm}^2 \text{ V}^{-1} \text{ sec}^{-1}$.

The mercury ionization frequency of plasma electrons is taken to be a fraction f_{ip} times the positive column value, which is D_a/Λ^2 , according to ambipolar diffusion theory of the positive column.^{2,3} The corresponding value of k_p is

$$k_p = \Lambda^{-1}(1 - f_{ip})^{1/2}.$$

Thus $f_{ip} = 1 \Rightarrow k_p = 0$ corresponds to the positive column.

III. RESULTS AND DISCUSSION

In this section, theoretical results of the preceding section are applied to the case investigated in Ref. 6—namely, a 0.4-A discharge in neon at 1 Torr and mercury at 6 mTorr contained in a tube of 3.6-cm i.d.¹⁷ These calculated results are based on the assumption $V_k = 15$ V.

Figure 2 shows predicted and measured plasma density plotted versus distance from the cathode, Fig. 3 shows predicted axial variation of electric field and plasma potential, and Fig. 4 shows predicted current densities of

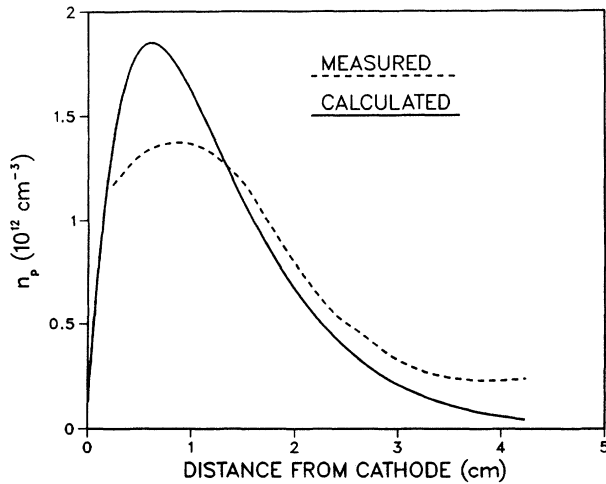


FIG. 2. Axial variation of plasma density $n_p(z)$ in the negative glow and Faraday dark space of a 0.4-A discharge in a cylindrical tube of 3.6-cm i.d. containing a mixture of neon at 1 Torr and mercury at 6 mTorr. Measurements from Ref. 6. Calculation of $n_p(z)$ according to Eq. (4) for $V_k = 15$ V, $\theta_e = 1.1$ V, $f_{ip} = 0.0$, $\Gamma_{b0} = I/\pi R_w^2 e = 2.46 \times 10^{17}$ cm $^{-2}$ sec $^{-1}$, and other parameters as designated in Sec. II C. Calculation stops at the end of the Faraday dark space where $L = 4.2$ cm.

beam electrons, plasma electrons, and ions. The curves in Figs. 2–4 are based on the following values for θ_e and f_{ip} , the two adjustable parameters: (1) $\theta_e = 1.1$ V; (2) $f_{ip} = 0$.

The value of 1.1 V for plasma electron temperature is taken from Ref. 6, and the value of zero for ionization frequency of plasma electrons is an arbitrary choice. While the choice of zero for f_{ip} may appear inconsistent with the choice of 1.1 V for θ_e , it can be argued that

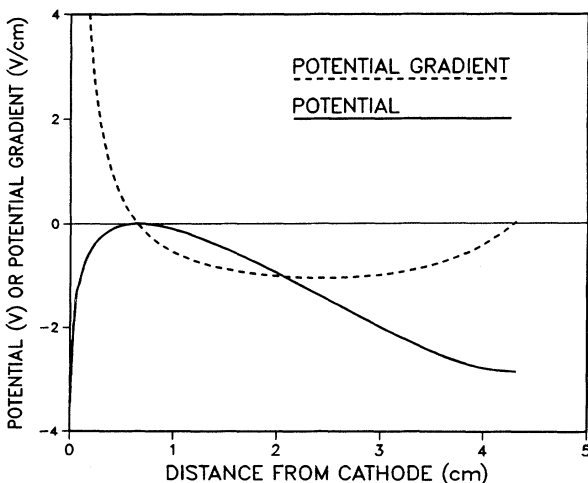


FIG. 3. Axial variation of electric field $E(z)$ and potential $V(z) \equiv \int_0^z E(z') dz'$. Calculation of $E(z)$ according to Eq. (3) for same discharge as Fig. 2. Calculations stop at the end of the Faraday dark space where $L = 4.2$ cm.

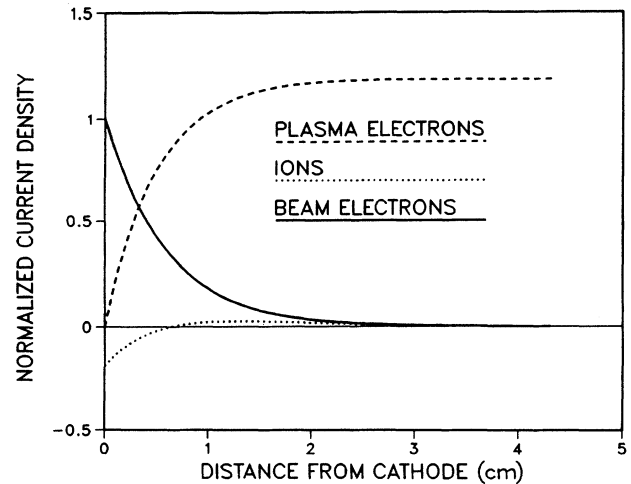


FIG. 4. Axial variation of normalized current densities of beam electrons, plasma electrons, and ions. Normalization factor is the emitted beam current density Γ_{b0} . Calculations according to Eqs. (1), (5), and (7) for the same discharge as Fig. 2. Calculations stop at the end of the Faraday dark space where $L = 4.2$ cm.

there is little or no ionization by plasma electrons because the tail of the energy distribution is depleted of high-energy electrons, as shown by electrostatic probe curves E and F in Fig. 9 of Ref. 6. With these choices, the combined length L of the NG plus FDS turns out to be 4.2 cm, and the ratio of ion current to electron current at the cathode G_{i0} , given by Eq. (7), is 0.22, both of which numbers are in good agreement with measurement.^{6,7} The combined length L of NG plus FDS was found by solving Eq. (5) for the value of L which satisfies $\Gamma_i(L) = 0$, as described previously.

A. Length of NG + FDS

This model predicts a combined length L of the NG + FDS close to that measured:⁶ calculated $L = 4.2$ cm, while measured $L = 4.3$ cm for the case of 1 Torr neon and 40°C wall temperature. According to the present model, the length L is determined by assumption 9—namely, that the ion current is zero at the end of FDS where the PC begins. Mathematically, L is determined from Eq. (5) by setting $\Gamma_i(L) = 0$. Physically, L corresponds to the place where most of the electrons and ions generated in the NG have been lost by ambipolar diffusion to the wall, and too few remain to support lamp current by ambipolar diffusion in the axial direction.

B. Plasma density and potential profiles

This model predicts plasma density profiles that are similar in shape to those measured,¹⁷ but the predicted peak value is somewhat higher than the measured peak value, as shown in Fig. 2. Predicted profiles of plasma potential are in qualitative agreement with observation, but the predicted locations of the two field reversals are

not in good agreement with observation. Absolute value of plasma potential depends on the value of plasma electron temperature, which is measured to be about 1.1 V.⁶ According to Fig. 3, the potential of the PC end of the FDS is predicted to be about 3 V below the maximum potential in the NG. This value is almost twice as high as the measured value of 1.7 V indicated by the 40°C curve in Fig. 15 of Ref. 6.

C. Ion current to cathode

This model predicts the ratio of ion current to electron current at the cathode in qualitative agreement with observation. According to Eq. (7), the ratio of ion current to electron current at the cathode is given approximately by the relation

$$G_{i0} \approx \frac{f_{ib}\alpha_b}{\alpha_b + k_p} = \frac{v_{ib}}{v_{xb} + v_{ib} + [(v_{xb} + v_{ib})D_b k_p^2]^{1/2}}. \quad (8)$$

Based on calculated values $f_{ib}=0.37$, $\alpha_b=1.89$, $k_p=1.34$, which are derived in Sec. II C, this expression gives $G_{i0}=0.22$ for $V_k=15$ V, in qualitative agreement with measurement.¹⁸

The radial ambipolar diffusion current density to the insulating wall of the discharge tube is given approximately by the expression

$$J_{pr}(R_w) = -eD_a \left[\frac{\partial n_p}{\partial r} \right]_{r=R_w} \approx eD_a n_p(z) \frac{J_1(2.405)}{\Lambda},$$

where $J_1(2.405)=0.52$ is the value of the first-order Bessel function of the first kind at the first zero of J_0 . Evaluation of this expression at the peak plasma density of 1.8×10^{12} cm⁻³ gives $J_{pr}(R_w) \approx 1$ mA/cm². Thus, radial ion-current density is much smaller than axial ion-current density to the cathode, which is G_{i0} times the thermionic current density emitted by the cathode. The latter may be as high as 10 A cm⁻².

Theoretical results for dimensionless current densities G_e , G_i , and G_b , defined as the ratio of current density to emitted beam current density, are shown in Fig. 4. Note that ion-current density is negative for distance less than 0.6 cm, positive for distance greater than 0.6 cm, and falls to zero at distance equal to 4.2 cm. Total current, which is the sum $G_b + G_e - G_i = 1 - G_{i0}$, is constant independent of position.

D. Field reversals in the NG and FDS

Figure 3 shows that there are two field reversals—one in the NG and one in the FDS, in agreement with observation.⁶ The field reversal closer to the cathode occurs because axial current can be carried by ambipolar diffusion due to a large axial density gradient, requiring no electric field except that due to the slight positive

space charge in the plasma, which actually retards axial electron motion. The second field reversal occurs near the end of the FDS, where the density of plasma electrons has fallen too low, due to radial diffusion losses, to carry axial current by ambipolar diffusion, causing the field to increase to carry the current. At the beginning of the PC, the field rises rapidly to the PC value, which is 0.5–2 V/cm in a typical mercury plus rare-gas discharge in a cylindrical tube of a few cm in diameter.

Predicted locations of the two field reversals relative to the cathode and beginning of the PC are not in good agreement with observation. Predicted field reversal near the PC occurs very near the end of the FDS, while observed field reversal occurs near the beginning of the FDS, as shown in Fig. 15 of Ref. 6. Predicted field reversal near the cathode occurs in the NG just after zero gradient in plasma density, while observed field reversal occurs so close to the cathode that its position cannot be determined by Langmuir probe measurements of plasma potential, as shown in Fig. 15 of Ref. 6. This observation is difficult to reconcile with the present ambipolar diffusion theory of the negative glow. The continuity equations for beam electrons, plasma electrons, and ions can be combined to give the following relation for the total current density Γ , which is independent of axial position:

$$\Gamma = \Gamma_b + \Gamma_e - \Gamma_i = \Gamma_{b0} - \Gamma_{i0}.$$

By Eqs. (1) and (2), this equation becomes

$$\Gamma = \Gamma_{b0} \exp(-\alpha_b z) - (\mu_e \theta_e - \mu_i \theta_i) \frac{dn_p}{dz} + (\mu_e + \mu_i) n_p E,$$

according to which the following conditions apply.

(1) The potential gradient must be positive to carry current in the axial direction at the location where the plasma density gradient is zero, provided that the beam electron current is small.

(2) The plasma density gradient must be negative to carry the current in the axial direction at the location where the potential gradient is zero, provided that the beam electron current is small.

Neither of these requirements is satisfied by the measurements of Ref. 6. Perhaps the difference between prediction and observation should be attributed to oversimplification of the present one-dimensional treatment in the vicinity of the cathode. The present model is based on the assumption of cylindrical geometry with a planar cathode, whereas the cathode in the experimental discharge tube of Ref. 6 is a stick about 0.1 cm in diameter and 1.5 cm long, placed perpendicularly to the axis of the discharge tube, which is 3.6-cm i.d.

IV. SUMMARY

Ambipolar diffusion theory of the negative glow and Faraday dark space of a cylindrical gas discharge maintained by thermionic emission from a hot cathode is discussed. Radial diffusion losses are handled by introducing the usual diffusion length. Inputs to the model are the following: thermionic current density emitted by the cathode; discharge tube radius; probability of ionization

by beam electrons; probability of ionization by plasma electrons; plasma electron and ion temperatures and mobilities. It is found that the negative glow can be maintained by beam electrons without ionization by plasma electrons. The model predicts combined length of the negative glow and Faraday dark space in good agreement with measurement. In addition, the model closely predicts the shape of measured axial distribution of plasma electron density. The model also predicts ion current to the cathode in qualitative agreement with observation. This ion current is much larger than the radial ambipolar diffusion current density at the insulating wall of the discharge. The model also predicts two reversals in the axial electric field—one in the negative glow near the

cathode where axial current is supported by ambipolar diffusion, and one end of the Faraday dark space at the beginning of the positive column where axial current can no longer be supported by ambipolar diffusion.

ACKNOWLEDGMENTS

The author would like to acknowledge Professor H. J. Oskam for valuable and constructive criticism of this work. The author would also like to thank J. F. Waymouth for supplying unpublished information about the experiments described in Ref. 6, for permission to use Fig. 4.2 of Ref. 7, and for reviewing the manuscript.

¹M. J. Druyvesteyn and F. M. Penning, *Rev. Mod. Phys.* **12**, 87 (1940), Sect. VII-B.

²W. Schottky, *Phys. Z.* **25**, 635 (1924).

³G. Francis, in *The Glow Discharge at Low Pressure*, Vol. 22 of *Handbuch der Physik*, edited by S. Flugge (Springer, Berlin, 1956), p. 53.

⁴J. H. Ingold, *Phys. Fluids* **15**, 75 (1972).

⁵L. Spitzer, *The Physics of Fully Ionized Gases* (Wiley Interscience, New York, 1956).

⁶J. F. Waymouth, *J. Appl. Phys.* **30**, 1404 (1959).

⁷J. F. Waymouth, *Electric Discharge Lamps* (MIT Press, Cambridge, MA, 1971), Chap. 4.

⁸W. Verweij, *Philips Res. Rep. Suppl.* 2 (1961).

⁹J. H. Ingold, *Phys. Rev. A* **40**, 7158 (1989).

¹⁰D. Bohm, in *The Characteristics of Electrical Discharges in Magnetic Fields*, edited by A. Guthrie and R. F. Wakerling (McGraw-Hill, New York, 1949), Chap. 3. It is customary to equate ion velocity at the edge of a collisionless sheath to the Bohm velocity v_B .

¹¹It is shown in Sec. II B 2 that the assumption of zero plasma density at the beginning of the NG leads to the same results as assumption 7.

¹²The present model has no positive column; in principle, therefore, the discharge extends axially to infinity. However, the present analysis is not applicable past the point where axial ion-current density goes to zero, because there is no ion

source beyond this point.

¹³T. J. Jones, *Phys. Rev.* **29**, 822 (1927).

¹⁴S. D. Rockwood, *Phys. Rev. A* **8**, 2348 (1973).

¹⁵L. G. H. Huxley and R. W. Crompton, *The Diffusion and Drift of Electrons in Gases* (Wiley, New York, 1974), Table 14.4 and Fig. 14.5.

¹⁶L. M. Chanin and M. A. Biondi, *Phys. Rev.* **107**, 1219 (1957).

¹⁷In a personal communication from J. F. Waymouth the author was informed that the discharge tube i.d. was 3.6 cm and the discharge current was 400 mA in the experiments described in Ref. 6. Likewise, the author was informed that the size of the probe used in the experiments of Ref. 6 was such that measured values of electron density were reduced by about 40% from the unperturbed values, making the measured value of peak, radially averaged, electron density equal to $1.25 \times 10^{12} \times 0.437/0.4 = 1.37 \times 10^{12} \text{ cm}^{-3}$. The factor 0.437 is the average value of the zero-order Bessel function of the first kind, and the peak value of measured density, $1.25 \times 10^{12} \text{ cm}^{-3}$, is obtained from Fig. 14 of Ref. 6 for $T_w = 40^\circ\text{C}$.

¹⁸J. F. Waymouth, *Electric Discharge Lamps* (Ref. 7), Chap. 4. See Fig. 4.7(b) to estimate the CF at about 15 V, and Fig. 4.13 to estimate the current ratio at about 0.15 for a CF of 15 V. The reader should be aware that the caption of Fig. 4.13 notes that the buffer gas in these measurements is neon with 10% argon and the wall temperature is only 20°C , not pure neon and 40°C , respectively, as in the measurements of Fig. 4.7.